Numerical Study on Correlation of Heat Transfer Coefficient with Void Fraction at Heat Transfer Tube Surface in Sodium Water Reaction

Toshinori MATSUMOTO, Takashi TAKATA and Akira YAMAGUCHI
Department of Energy and Environment Engineering, Osaka University
2-1 Yamada Oka, Suita, Osaka, Japan 565-0871
matsumoto_t@qe.see.eng.osaka-u.ac.jp, takata_t@see.eng.osaka-u.ac.jp,
yamaguchi@see.eng.osaka-u.ac.jp

Akikazu KURIHARA, Hiroyuki OHSHIMA
Japan Atomic Energy Agency
4002, Narita, O-arai, Higashi-Ibaraki, Ibaraki, Japan

ABSTRACT

The present paper deals with a sodium water reaction (SWR) in a steam generator (SG) of sodium-cooled fast reactor (SFR). When a heat transfer tube in the SG fails, SWR would take place. This reaction occurs rapidly and accompanies a high temperature jet. This jet would cover up the neighboring tubes and the tubes have possibilities to fail secondarily by an overheated rupture. Therefore, the quantification of the heat transfer from the fluid to the tube in the SWR is important from the view point of safety evaluation. To obtain knowledge on the SWR phenomenon, experiments with SWAT-1R test facility were carried out at Japan Atomic Energy Agency (JAEA). In the experiment, thermocouples were installed at 6 locations on a tube placed for measurement in the SWR reacting zone and the temperature histories were measured.
In the present study, the heat transfer coefficient has been evaluated by solving one-dimensional inverse problem of heat transfer based on the SWAT-1R experimental result. And the flow characteristics such as a void fraction and a fluid velocity, at the surface of the heat transfer tube have been speculated from the magnitude of heat transfer coefficient.
Furthermore, one-dimensional thermal hydraulics simulation has been performed based on a boundary layer approximation. In the analyses, the fluid velocity at out of the boundary layer and the void fraction condition are given as a parameter. As a result, the correlation diagram between the heat transfer coefficient and the flow characteristics has been evaluated so as to investigate the flow characteristics in the SWAT-1R experiment.

KEYWORDS

Sodium Water Reaction, Over Heating Rupture, Heat Transfer Coefficient, Sodium Cooled Fast Reactor, Steam Generator, Void Fraction

1. INTRODUCTION

In the steam generator (SG) of a fast breeder reactor, liquid sodium is supposed to be the coolant. In the SG, heat transfer tubes are placed in helical coil shape. Water flows inside of the tubes, and exchange the heat with liquid sodium that flows in the shell side. When a tube fails, water vapor would leak into sodium. After the failure of the heat transfer tube in the SG, the sodium water reaction (SWR) starts with the contact of water vapor with liquid sodium.

Sodium water reaction generates heat and the rate of reaction is rapid. In the reaction jet, the droplets of sodium or chemical reaction products would collide with the tube surface. Therefore, the surface of the heat transfer tubes would be deteriorated. Furthermore, heat transfer tubes in the reaction region would be heated up by the high temperature environment. Therefore, the material has possibilities of secondary failure because of the deterioration of the material strength by erosion, corrosion or over heating. Secondary failure caused by over-heating is called over-heating rupture.

SWR failure propagation tests with the SG safety test facility, SWAT-3[1] have been conducted at Japan Atomic Energy Agency (JAEA). In the tests, the over-heating rupture has not been observed in the actual condition of SG of 'Monju: Japanese prototype SFR'. However, the larger size or higher temperature SG is focused for efficiency of SFR. In that condition, there is a strong possibility of the over-heating rupture. With this reason, the evaluation of the over-heating rupture of heat transfer tube in SG in the SWR region is needed.

To evaluate the possibility of the secondary failure in case of over-heating rupture, estimation of the heat transfer from the fluid to the tube wall during the SWR region is significant. Amount of the heat transfer can be evaluated by introducing heat transfer coefficient on the surface of the tube. The heat transfer coefficient reflects flow characteristics including distribution of fluid velocity, void fraction and temperature. Furthermore, such as alignment of the tubes also have effects on the heat transfer coefficient. The heat transfer coefficient can be calculated numerically with the distribution of the temperature of the fluid and the tube.

SWAT-1R is an experimental apparatus of JAEA [2]. SWR is taken place in the test section. On a certain tube, thermocouples are aligned to measure distribution of temperature transient of fluid and the tube wall.

In the present study, non-stationary heat transfer coefficient of a heat transfer tube in the SWR region has been analyzed numerically based on the experimental data obtained with SWAT-1R as the boundary condition. The flow characteristics around the heat transfer tube during the SWR have been estimated with the heat transfer coefficient obtained from the computation. In the estimation, it is inferred that the transient of the heat transfer coefficient relies on the void fraction.

Therefore, the thermal hydraulic simulation of the fluid around the tube is conducted. The heat transfer coefficient is computed by setting the velocity and the void fraction at the fluid as parameters. As the result, the correlation diagram between the heat transfer coefficient and the void fraction has been obtained in each velocity conditions. With the correlation diagram, the void fraction around the heat transfer tube in the SWR has been evaluated.

2. SWAT-1R EXPERIMENT

Figure 1 shows the test section in the reaction vessel of SWAT-1R. The test section consists of 43 dummy tubes that mock up the heat transfer tubes of SG in Japanese prototype SFR 'Monju'. These tubes consist of 2-1/4Cr-1Mo steel. Diameter and the thickness of tubes are the real scale. Water vapor flows out from the water vapor injection tube located in the lower part in the test section. The measurement tube is placed at approximately 100 mm above the failed tube. In this study, temperature histories in an experiment have been applied as the boundary condition.

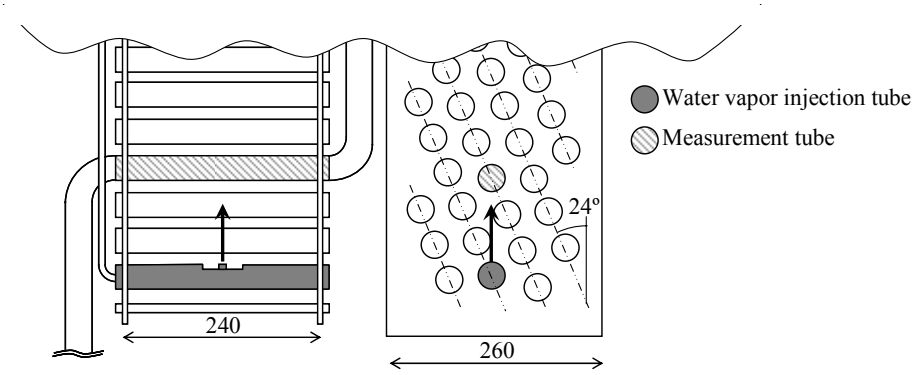

Fig. 1 Test section of SWAT-1R.

The test section is filled with stagnant liquid sodium in the initial condition. The outer diameter of the measurement tube is 31.8 mm and the thickness is 3.8 mm. The tube for leakage has the water vapor nozzle which diameter is 5.8 mm. Inside of this tube, high pressure and high temperature water vapor flows. In the SWR experiment, the leak rate was set to 0.3 kg/s. The leakage lasted for 30 seconds. Water vapor was blown out upward from the nozzle. Pressure inside of the reaction vessel is supposed to be 0.05 MPa·G ~ 0.1 MPa·G. After 5 seconds of the leakage starts, a rupture disk broke to keep the vessel pressure below an allowable level and then the pressure decreased to 0.015 MPa·G during this experiment.

To obtain the temperature transient in the fluid and the tube wall, thermocouples (T/Cs) are arranged in three axial locations as shown in the left of Fig. 2. Locations B and E are right above the water vapor injection nozzle. Locations A, D and C, F are located in 50 mm away from Locations B and E in the axial direction. Locations A, B and C are located at the bottom side of the tube, and Locations D, E and F are located at the opposite side (top side). Exact positions of T/Cs are shown in the drawing right of Fig. 2. In every Locations, one T/C is arranged at 2 mm from the tube surface (Point a). Another two T/Cs are embedded inside the tube wall (Point b and c). In each Point, temperature time histories were measured during the experiment.

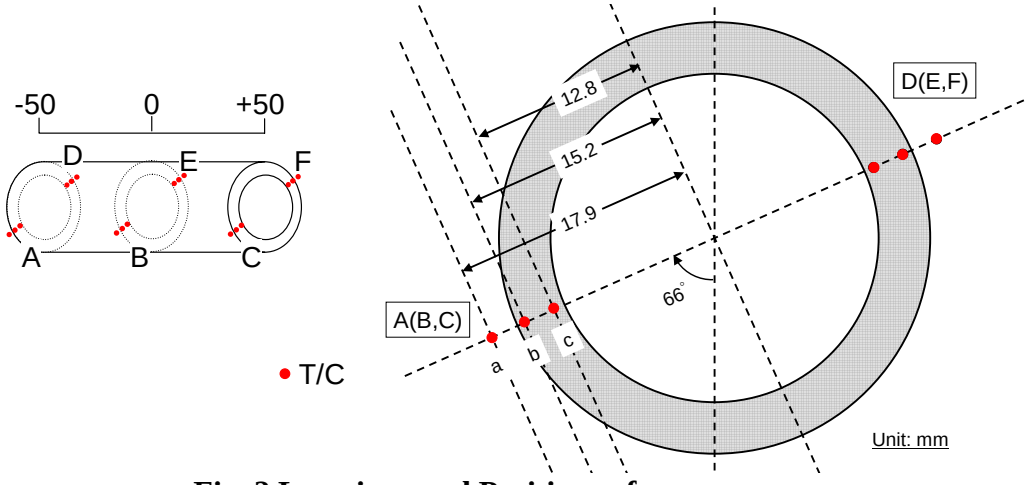

Fig. 2 Locations and Positions of measurement.

3. ANALYSIS OF HEAT TRANSFER COEFFICIENT

Numerical investigation of heat transfer coefficient from the fluid to the heat transfer tube in the SWR has been carried out based on the temperature data measured in the experiment with SWAT-1R. The heat transfer coefficient has been evaluated by solving the governing equations inversely.

3.1 NUMERICAL METHOD

Temperature of the heat transfer tube is computed by solving one dimensional heat conduction equation in cylindrical coordinates. The governing equation is described as:

$$\rho C_p \frac{\partial T}{\partial t} = \frac{1}{r}\frac{\partial}{\partial r}\left(r\lambda \frac{\partial T}{\partial r} \right) \tag{1}$$

where λ, ρ and C_p are the thermal conductivity, the density, and the specific heat respectively. T, r and t are the temperature and the radial coordinate and the time respectively. Equation (1) is discretized based on a control volume of each computational cell. At the outer surface of the tube, a heat transfer coefficient is introduced to evaluate a heat flux between the heat transfer tube and the fluid.

In the experiment, the tube wall temperatures at Point b and c and the fluid temperature at Point a were measured in each Location (see Fig. 2). Therefore, the heat transfer coefficient can be evaluated by solving the discretized equations inversely. Temperature at Points a and c are used as boundary conditions, and the Point b is used as the reference condition. In each computational time step, temperature distribution is calculated with the discretized equations with the boundary conditions. Then the heat transfer coefficient is updated. With the new heat transfer coefficient, the temperature distribution is calculated iteratively. This iteration process is repeated until the temperature at Point b coincides with the experimental result in a convergence criterion.

3.3 RESULTS AND DISCUSSIONS

In the computation, time step is set to 0.05 seconds which is the same as the measurement interval in the experiment. Time duration is set to 35 seconds, because the measurement was carried out from 5 seconds before water injection to 30 seconds when the injection finished.

In the numerical investigation, physical properties of the tube material (2-1/4Cr-1Mo) are defined with the empirical correlation equations [3].

Heat transfer from fluid to the tube is expressed by introducing heat transfer coefficient on the surface of the tube. Heat transfer coefficient includes the influences of the radiation, convection and conduction of heat. Other elements which have influence to the heat transfer are also included, for instance, condition of the solid material, the characteristics of fluid (velocity, void fraction or temperature) and the alignment of the tubes. This indicates that the heat transfer coefficient reflects all kinds of flow characteristics. In other words, the heat transfer coefficient can be inferred if the flow characteristics are known.

Time history of non-stationary heat transfer coefficient of the heat transfer tube in SWR has been analyzed. Figure 3 shows the computed heat transfer coefficient and temperature trend

of the fluid side (Point a) at Location A as an instance. Here, it is noted that the heat transfer coefficient at Location B has not been evaluated because the impractical temperature was measured.

Tables 1 and 2 show the time-weighted average and the median value of the heat transfer coefficient at typical periods that is roughly divided according to the flow characteristics. At Location A, from 5 to 18 seconds, these two values are considerably different although they are consistent for 0 - 5 seconds. To clarify the difference between the time-weighted average and the median value, the temperature history of Point b at Location A has been evaluated. In this evaluation Mean heat transfer coefficients at Location A indicated in Table 1 are used as the heat transfer coefficient on the surface of the tube. Measured temperature histories at Point a and c are used as the boundary condition and that at Point b are calculated and compared with the experimental data. Figure 4 shows the result of computed temperature history at Point b of Location A. Temperature history with the median value follows the measured history well. In the history of the heat transfer coefficient, much extremely high value exists. When the time-weighted average is calculated, the extremely high values have effects. So the time-weighted average tends to be evaluated largely. Therefore, the median value is used as the mean value for the investigation of the flow characteristics in following discussion.

Table. 1 Mean heat transfer coefficient at Locations A and C

Location	Time (s)	h (W/m^2/K)	
		Time average	Median
A	0.0-2.0	28,000	34,000
	2.0-5.0	26,000	26,000
	5.0-18.0	95,000	42,000
	18.0-30.0	214,000	112,000
C	0.0-8.0	15,000	15,000
	8.0-17.0	27,000	25,000
	17.0-30.0	876,000	128,000

Table. 2 Mean heat transfer coefficient at Locations D, E and F

Location	Time (s)	h (W/m^2/K)	
		Time Average	Median
D	0.0-3.5	80,000	58,000
	3.5-30	22,000	20,000
E	0.0-5.0	219,000	51,000
	5.0-30.0	37,000	17,000
F	0.0-3.0	74,000	46,000
	3.0-30.0	20,000	16,000

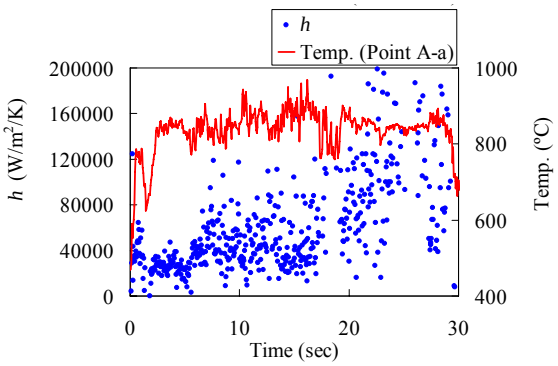

Fig. 3 Heat transfer coefficient at Location A

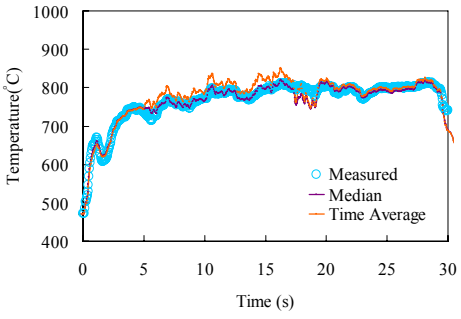

Fig. 4 Temperature history with the mean value at Point A-b

Flow characteristics in each Location have been investigated with the mean values of the heat transfer coefficient indicated in the Tables 1 and 2. At the first several seconds (0 to approximately 5 seconds), the reaction is starting and the jet collides with the tube. In this period, the mean heat transfer coefficient has been evaluated smaller than 30,000 W/m^2/K at the bottom side (Locations A and C). The value of the heat transfer coefficient at Location A is larger than C. Therefore, influence of liquid phase at Location A has been expected to be

stronger than Location C. On the other hand, the heat transfer coefficient at the top side (Locations D, E and F) has been evaluated approximately 50,000 W/m^2/K that is larger comparing with the bottom side. Consequently, it can be expected that the influence of gas phase at bottom side is stronger than the top side.

The heat transfer coefficient at Locations A and C has been increasing from 5 to 18 seconds. Hence it can be said that the influence of gas phase is decreasing. On the other hand, the heat transfer coefficient at Locations D, E and F has been evaluated smaller than 20,000 W/m^2/K. So it is expected that the gas phase covers up the top side. The heat transfer coefficient at Location D has been evaluated larger than F. Therefore, influence of liquid phase has been presumed to be stronger at Location D than F.

After 18 seconds, the heat transfer coefficient at Locations A and C has been evaluated over 100,000 W/m^2/K. This indicates that the heat transfer tube is surrounded by liquid phase. At Locations D, E and F, the heat transfer coefficient has been evaluated smaller than 20,000 W/m^2/K. Therefore it is expected that the fluid characteristics are the same as the period between 5 to 18 seconds.

4. CORRELATION DIAGRAM BETWEEN HEAT TRANSFER COEFFICIENT AND VOID FRACTION

In the previous section, the heat transfer coefficient on the surface of heat transfer tube in the SWR region has been analyzed numerically. Furthermore the flow characteristics have been investigated with the mean values of the heat transfer coefficient. Besides, the difference between the Locations and periods of time has been evaluated. It is expected that the rate of the gas or liquid phase, i.e. the void fraction make the difference.

To clarify the influence of the void fraction to the heat transfer coefficient, a correlation diagram has been developed in this section. According to the previous work [4] in which the numerical analysis of the SWAT-1R experiment, it can be presumed that the mixture gas around the surface of the heat transfer tube consists of hydrogen and liquid sodium. And the void fraction of hydrogen gas is more than 90%. Therefore it is assumed that the fluid consists of two phase (hydrogen gas and liquid sodium). Numerical analysis of two phases, 1-dimensional thermal hydraulic flow has been performed. Boundary layer approximation and the turbulence model have been applied. In this analysis, the boundary velocity and void fraction has been given as parameters. Furthermore, the relationship of the void fraction around the heat transfer tube during the SWR has been evaluated with the correlation diagram.

4.1 NUMERICAL METHOD

One-dimensional boundary layer approximation is applied [5]. In this theory, the tangential velocity(u_x) in the boundary layer using the boundary velocity(u_B) is given as:

$$u_x = u_B f' \tag{2}$$

where f' is space derivative of non-dimensional flow stream function.

With Reynolds average of conservation equations, the governing equations are described as:

Mass conservation equation:

$$\frac{u_B}{x} f' + u_B \frac{\partial f'}{\partial x} + \frac{\partial u_z}{\partial z} = 0 \tag{3}$$

Momentum conservation equation:

$$\frac{\partial f'}{\partial t} + u_B f' \frac{\partial f'}{\partial x} + u_z \frac{\partial f'}{\partial z} = \frac{\partial}{\partial z}\left[(\nu + \nu_t) \frac{\partial f'}{\partial z} \right] \tag{4}$$

Energy conservation equation:

$$\frac{\partial (\rho C_P T)}{\partial t} + u_B f' \frac{\partial (x \rho C_p T)}{\partial x} + u_z \frac{\partial (\rho C_p T)}{\partial z} = \frac{\partial}{\partial z}\left(\lambda \frac{\partial T}{\partial z} \right) - \frac{\partial}{\partial z}\left[\alpha_t \frac{\partial (\rho C_p T)}{\partial z} \right] \tag{5}$$

where t is the time. ρ, p and T mean the density, the pressure and the temperature of the mixture gas respectively. u_z is the velocity vertical to the wall. ν, λ and C_p are the dynamic viscosity, the heat conductivity and the specific heat of the mixture gas.

A low Reynolds number turbulence model is used in the numerical simulation code. Introducing the gradient-diffusion hypothesis, the Reynolds stress and the turbulent heat flux are defined using the turbulent viscosity ν_t and the turbulent thermal diffusivity α_t

In the low Reynolds number turbulence model [6], the equations for turbulence energy k and the energy dissipation ratio ε are given as:

Conservation of the turbulence energy:

$$\frac{\partial k}{\partial t} + u_B f' \frac{\partial k}{\partial x} + u_z \frac{\partial k}{\partial z} = \frac{\partial}{\partial z}\left[\left(\nu + \frac{\nu_t}{\sigma_t} \right) \frac{\partial k}{\partial z} \right] + \nu_t \left(u_B \frac{\partial f'}{\partial z} \right)^2 - \varepsilon \tag{6}$$

Conservation of the turbulence energy dissipation ratio:

$$\frac{\partial \varepsilon}{\partial t} + u_B f' \frac{\partial \varepsilon}{\partial x} + u_z \frac{\partial \varepsilon}{\partial z} = \frac{\partial}{\partial z}\left[\left(\nu + \frac{\nu_t}{\sigma_t} \right) \frac{\partial \varepsilon}{\partial z} \right] + \left(C_1 \nu_t \left(u_B \frac{\partial f'}{\partial z} \right)^2 - C_2 \varepsilon \right) \frac{1}{\tau} + \nu \nu_t \left(u_B \frac{\partial^2 f'}{\partial z^2} \right)^2 \tag{7}$$

To calculate the thermal conductivity of the mixture gas, the Davis's equation [7] is used. The equation is described as:

$$\lambda_e / \lambda = 1 + \frac{3(k-1)}{k+2-(k-1)(1-\alpha)} [(1-\alpha) + f(k)(1-\alpha)^2 + O((1-\alpha)^3)] \tag{8}$$

where λ_e is the effective thermal conductivity, λ is the thermal conductivity of the gas phase, k is the ratio of the thermal conductivity of the liquid sodium to λ, and α is the void fraction. The function $f(\alpha)$ approaches 0.5 if the void fraction is large.

4.2 RESULTS AND DISCUSSIONS

In this section, the heat transfer coefficient is numerically evaluated as a function of the void fraction. Let us assume the geometry of SWAT-1R and the T/Cs locations shown in Fig. 2.

The boundary condition is defined at Point a and c. The temperatures are 900 ºC and 500 ºC respectively. Velocity at Point a is either 1.0 m/s or 1.5 m/s to investigate the influence of the flow velocity outside of the boundary layer.

Figure 5 shows the correlation diagram between the heat transfer coefficient and the void fraction obtained from the computation. The difference of the boundary velocity appears in the diagram.

The void fraction can be estimated using the correlation diagram, if we know the heat transfer coefficient. Let us show an example of the inference. Figure 6 shows the heat transfer coefficient as a function of the void fraction when u_B = 1.0 m/s. We over plot the heat transfer coefficient at Location A given in Table 1. From this figure, we can see the void fraction is approximately 0.7 at the first 2 seconds on the assumption that the velocity at Point a is 1.0 m/s. Beyond the time period, the void fraction is evaluated to be 0.74 at 2 to 5 seconds, 0.68 at 5 to 18 seconds and 0.4 at 18 to 30 seconds, respectively. It seems that the estimation in the previous section is consistent with the void fraction estimation shown in this section.

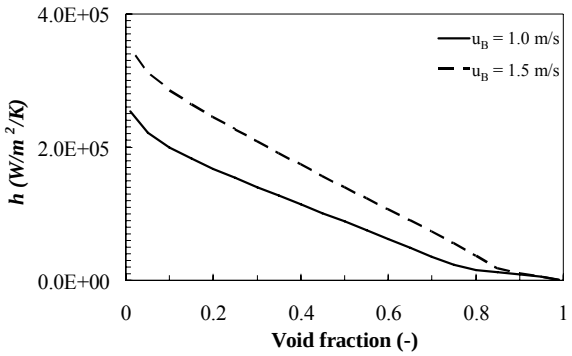

Fig. 5 Correlation diagram of heat transfer coefficient and void fraction

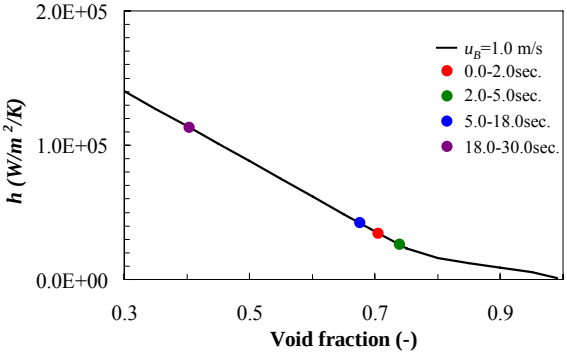

Fig. 6 Evaluation of void fraction

The histories of void fraction have also been calculated with the diagram (u_B = 1.0 m/s). The heat transfer coefficient histories at Locations A, C and D, F have been applied. In the calculation, the heat transfer coefficient outlying the correlation diagram has been eliminated. Figure 7 shows the transient of void fractions at Locations A and C (bottom side), and Fig.8 shows the transient of void fraction at Locations D and F (top side).

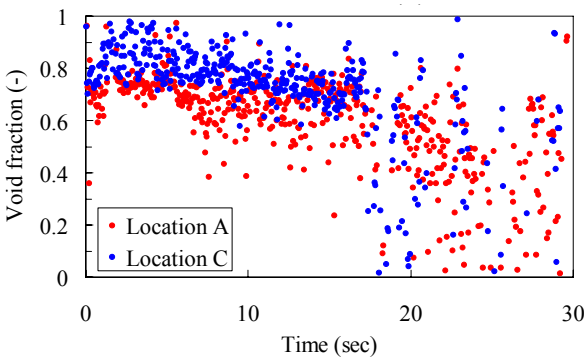

Fig. 7 Transient of Void fraction (bottom side)

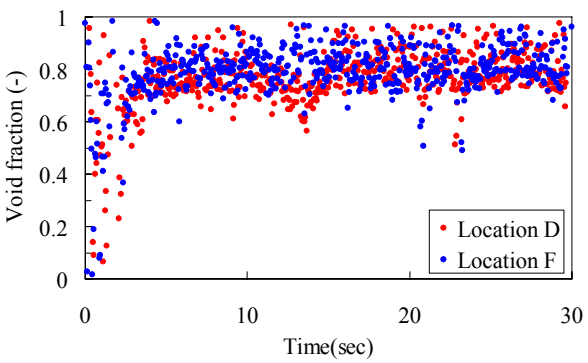

Fig. 8 Transient of Void fraction (top side)

Flow characteristics investigated from Figures 7 and 8 are indicated with images around the heat transfer tube. Figure 9 shows the image of the SWR jet in the initial several seconds. In this period, the reaction gas will collide with the bottom side firstly. Therefore, the void fraction at bottom side has been evaluated larger comparing with the top side. At the top side, the void fraction in the first several seconds is considerably fluctuated. Hence, it can be expected that the liquid phase had strong influence. As seen in Fig. 7 until 18 seconds in the experiment, it seems that the void fraction at Location A has been evaluated smaller than Location C as like as the previous section. At top side, however, clear difference between Location D and F has not appeared, in contrast to the previous section.

Figure 10 indicates the broadening of the SWR gas region in the period of 5 to 18 seconds. Although the heat transfer coefficients at the Locations A and C shown in Fig. 3 are increasing and fluctuated during 5 to 18 sec., the void fraction shown in Fig. 7 has been evaluated approximately 0.6. So the gas phase is expected to covers up these Locations in this period. On the other hand, the void fraction has been evaluated approximately 0.8 at the top side in Fig. 8. In this period, it is expected that the gas region covers up the tube.

After 18 seconds, the void fraction at the bottom side is fluctuated and decreasing as shown in Fig.7. In this period, the temperature at Location C tends to fall below the boiling point of the sodium, so it can be expected that considerably strong influence of the liquid sodium exist at the bottom side. Alternatively, it can be expected that the gas region lean toward the one side in which the top side exists when the SWR jet collide with the tube. Therefore it has been assumed that the liquid phase was covering up the Location A and C in this period. Figure 11 shows the sketch of the flow characteristics.

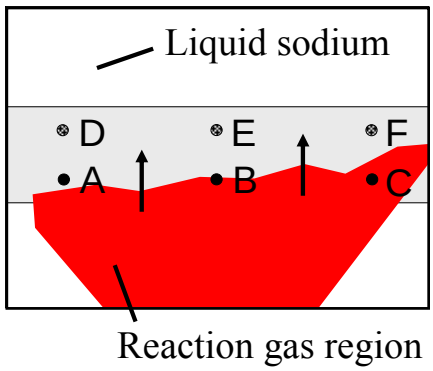

Fig. 9 Image of SWR jet (0 to 5 sec.)

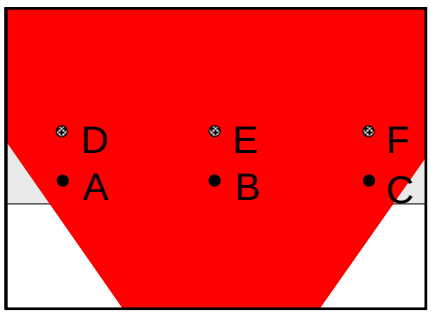

Fig . 10 Image of SWR jet (5 to 18 sec.)

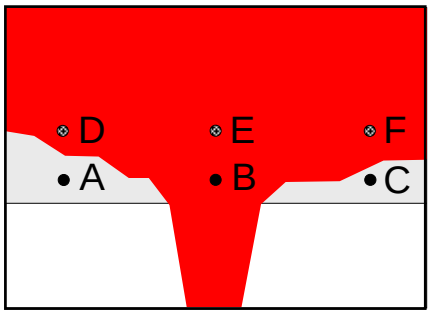

Fig. 11 Image of SWR jet (18 to 30 sec.)

In this section, the correlation diagram between the heat transfer coefficient and the void fraction has been evaluated. With this diagram, the transient of void fraction during the SWR

has been evaluated. However the boundary velocity has been set to constant value as an assumption in the computation. For clearer evaluation of the flow characteristics around the heat transfer tube during the SWR, it is recommended that the evaluation based on the multi-dimensional thermal hydraulic flow analysis.

5. CONCLUSIONS

In the present study, the heat transfer coefficient of the heat transfer tube in the SWR region is obtained based on the numerical investigation. In this investigation, the temperature data measured in the SWAT-1R experiment has been used. One-dimensional heat transfer conduction and the heat transfer coefficient on the surface of the heat tube are assumed. An inverse problem is solved to obtain the heat transfer coefficient.

The mean values of the heat transfer coefficient histories are calculated in several periods. The flow characteristics around the heat transfer tube during the SWAT-1R experiment has been evaluated considering the mean values. As the result, it has been indicated that the transient of the heat transfer coefficient reflects the transient of the void fraction.

To see the influence of the heat transfer coefficient to the void fraction, the numerical analysis based on the two phase thermal hydraulic flow has been carried out. In this analysis, one-dimensional boundary layer approximation has been applied. The velocity and the void fraction in fluid have been set parametrically as the boundary conditions. The heat transfer coefficient in each condition has been computed. As the result the correlation diagram between the heat transfer coefficient and the void fraction has been evaluated. The difference of the boundary velocity appears in the correlation diagram. Furthermore, the flow characteristics of the fluid around the heat transfer tube are estimated. The histories of the void fraction have been obtained by applying the histories of the heat transfer coefficient to the correlation diagram. The images of the flow characteristics of the fluid have also been indicated.

To estimate the flow characteristics of the fluid around the heat transfer tube in the SWR region accuracy, it is needed that the multi-dimensional thermal hydraulic analysis.

REFERENCES

1. Osamu, M et al, *The Development and Application of Overheating Failure Model of FBR Steam Generator Tubes (IV),* JNC TN2400 2003-003, JNC Engineering report (2004)
2. Nishimura, M et al, *Sodium-water reaction test to thermal influence on heat transfer tubes, JNC TN9400 2003-014,* JNC Engineering report (2003)
3. Takasu, H et al *Physical Properties for Sodium Technology (Na, Ar, He, 304SS, 316SS, 21/4Cr-1Mo,* PNC N941 81-7, PNC technical paper3 (1981)
4. Takata, T et al, *Numerical Methodology of Sodium-Water Reaction with Multi-Phase Flow Analysis, Nucl. Sci. and Engineering*, **150**, 221-236, (2005)
5. Yamaguchi, A et al, *Thermal Influence on steam generator heat transfer tube during sodium-water reaction accident of sodium-cooled fast reactor,* NURETH-12, (2007)
6. Yang, Z et al, *New time scale based k-e model for nearwall turbulence, AIAA Journal*, **31**, 1191-1198 (1993)
7. R.H.Davis, *The Effective Thermal Conductivity of a Composite Material with Spherical Inclusions, International Journal of Thermophysics*, **7**, **3** (1986)